Particle transport and fluctuation characteristics around neoclassically optimized configurations in LHD

K. Tanaka, C. Michael, [a]L. N. Vyacheslavov, M. Yokoyama, [b]S. Murakami, [c]A. Wakasa, [d]H. Takenaga, [e]K. Muraoka, K. Kawahata, T. Tokuzawa, T. Akiyama, K. Ida, M. Yoshinuma, I. Yamada, K. Narihara, H. Yamada and the LHD Experimental group

National Institute for Fusion Science,322-6 Oroshi-cho, Toki 509-5292, Japan

[a]Budker Institute of Nuclear Physics, 630090 Nobosibirsk, Russia

[b]Department of Nuclear Engineering, Kyoto Univ., Kyoto 606-8501, Japan

[c]Graduate School of Engineering, Hokkaido Univ., Sapporo 060-8628, Japan

[d] Japan Atomic Energy Agency, 801-1, Mukoyama, Naka 311-0193, Japan

[e]School of Engineering, Chubu Univ., Kasugai 487-8501, Japan

Density profiles in LHD were measured and particle transport coefficients were estimated from density modulation experiments in LHD. The data set contains the wide region of discharge condition. The dataset of different magnetic axis, toroidal magnetic filed and heating power provided data set of widely scanned neoclassical transport. At minimized neoclassical transport configuration in the dataset (Rax=3.5m, Bt=2.8T) showed peaked density profile. Its peaking factor increased gradually with decrease of collisional frequency. This is a similar result observed in tokamak data base. At other configuration, peaking factor reduced with decrease of collsional frequency. Data set showed that larger contribution of neoclassical transport produced hollowed density profile. Comparison between neoclassical and experimental estimated particle diffusivity showed different minimum condition. This suggests neoclassical optimization is not same as anomalous optimization. Clear difference of spatial profile of turbulence was observed between hollowed and peaked density profiles. Major part of fluctuation existed in the unstable region of linear growth rate of ion temperature gradient mode.

Keywords: density profile, peaking factor, density modulation experiments, neoclassical transport, anomalous transport, diffusion coefficient, convection velocity, phase contrast imaging, turbulence

1. Introduction

Optimization of magnetic configuration for reducing energy and particle transports is an important issue for studies in stellarator/heliotron devices. In LHD, magnetic properties can be changed by scanning magnetic axis positions then systematic studies of the effects of magnetic configuration on transports are possible. Optimized configuration for reducing neoclassical transport was studied for R_{ax}=3.5~3.75m using the DCOM code and was found that the neoclassical transport was to be minimum at R_{ax}=3.5m in the plateau regime and at R_{ax}=3.53m in the 1/ν regime [1]. Then, it was experimentally observed that the effective helical ripple, which is an influential parameter of neoclassical transport in the 1/ν regime, played an important role on global energy confinement [2]. Inter machine studies show smaller effective helical ripple configuration showed higher enhancement of global energy confinements compared with international stellarator scaling 2005 [2]. This suggests that neoclassical optimization may also affect anomalous transport because transport in the data set of [2] was dominated by anomalous transport. In the previous work, systematic studies of particle transport and fluctuation properties were carried out at R_{ax}=3.6~3.9 m [3,4]. Particle diffusion was found to be anomalous and the smaller at the more inward shifted configuration. Simultaneously, the smaller fluctuation level was observed. Density profiles were hollow in many case of discharge, and became peaked ones at higher magnetic fields at higher collisionality. When density profiles were hollow, particle convection was comparable with that from the neoclassical prediction.

In this article, particle transports were studied at around optimized neoclassical configuration in order to investigate linkage between neoclassical and anomalous

author's e-mail: ktanakal@nifs.ac.jp

transport.

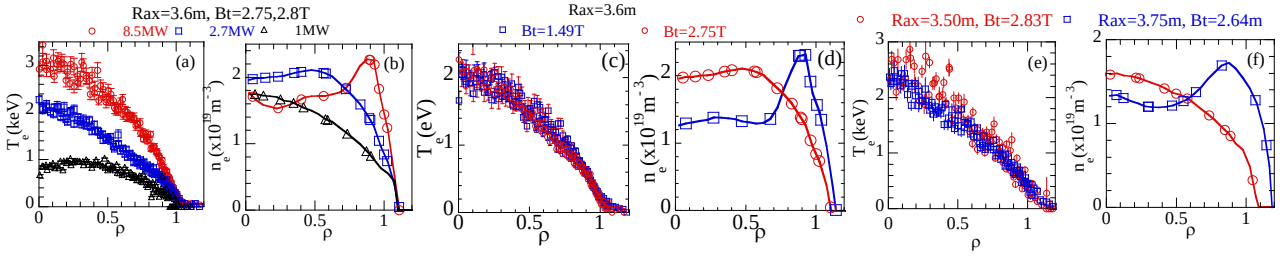

Fig.1 Comparison of (a), (c), (e) T_e and (b), (d), (f) n_e profiles under different condition. (a), (b) different NBI power, (c), (d) different magnetic field (e), (f) different magnetic configuration (Rax=3.5m and 3.75m is reduced and enhanced helical ripple configuration respectively

2. Experimental results

2.1 General character of density profile in LHD

Figure 1 shows electron temperature (T_e) and electron density (n_e) profiles under various conditions. The density profiles were measured by multi channel far-infrared interferometer [5] and electron temperature profiles were measured by YAG Thomson scattering [6]. The density profiles vary depending o the discharge condition. This is clear contrast to tokamak density profiles, which are peaked in the most of the case [7, 8]. Density profile changes from peaked one to hollow one with increasing of heating power as shown in Fig. 1 (b). With higher heating power, steeper T_e gradient was formed. This higher Te gradient can cause outward convective flux [3]. Figure 1 (c) and (d) show T_e and n_e profiles under different toroidal magnetic field (Bt) with almost identical T_e profiles. The toroidal magnetic field is also can affects the density profile. The density profiles became more hollow at lower magnetic field. The magnetic configuration can affect density profile as well. As shown in Fig.1 (f), at more outward configuration, density profiles tend to be hollow. Magnetic axis position were also influential parameter on density porofile.

Figure 2 shows parameter dependence of density peaking factor. The density peaking factor was defined as the ratio between the density at ρ (normalized radius) =0.2 and volume averaged density. The volume averaged density was calculated within the last closed flux surface. Figure 2 (a) shows comparison of dependence on ν_b^*, which is normalized by the collisional frequency at plateau and banana regime and defined by the following equation.

$$\nu^*_b = \nu_{ei}/(\varepsilon_t^{3/2}\nu_T/qR) \qquad (1)$$

where ε_t is an inverse aspect ratio, ν_T is an electron thermal velocity, q is a safety factor and R is a major radius. In the single helicity stellarator, the boundary of plateau and banana region can be defined [9]. LHD is multiple helicity configuration, however, for the comparison with JT60U elmy H mode data, ν_b^* was used. In JT60U, the peaking factor increases with decrease of ν_b^*. This is widely observed in tokamak [7,8]. In LHD, density peaking gradually increased with decrease of ν_b^* at Rax=3.5m, Bt=2.8T only. At other configuration (Rax=3.6m in Bt=2.75,2.8T, Rax=3.75m in Bt=2.64T and Rax=3.9m, Bt=2.54T), the density peaking factor reduced with decrease of ν_b^*. This is an opposite tendency to tokamak.

The data in Fig.2 are from NBI heated plasma, however, particle fueling from the NBI did not affect density peaking in both JT60U and LHD [3,4,7]. The variations of density profiles are not due to the difference of particle fueling but due to the difference of transport. Figure 2(a) suggests there is a common physics mechanism to determine density profile in JT60U and Rax=3.5m, Bt=2.8T in LHD, but there are different mechanism in other configuration of LHD.

Figure 2 (b) and (c) show dependence on normalized collision frequency (νh*) of the stellarator/helical configurations, which is defined as following equation.

$$\nu^*_h = \nu_{ei}/(\varepsilon_{eff}^{3/2}\nu_T/qR) \qquad (2)$$

where ε_{eff} is an effective helical ripple, which represents multiple helicity and is defined as [10],

$$\varepsilon_{eff} = \left(\frac{9\sqrt{2}}{16}\frac{\nu}{\nu_d^2}D\right)^{2/3} \qquad (3)$$

where ν, ν_d and D are the collision frequency, the drift velocity and the particle diffusivity in the enhanced helical ripple trapped region (the 1/ν region), respectively. At the upper boundary of the 1/ν region, ν^*_h becomes around unity.

As shown in Fig.2 (b), (c), the density peaking factor reduced with decrease of ν^*_h. Also, configuration dependence on ν^*_h became clear compared with Fig.2 (a).

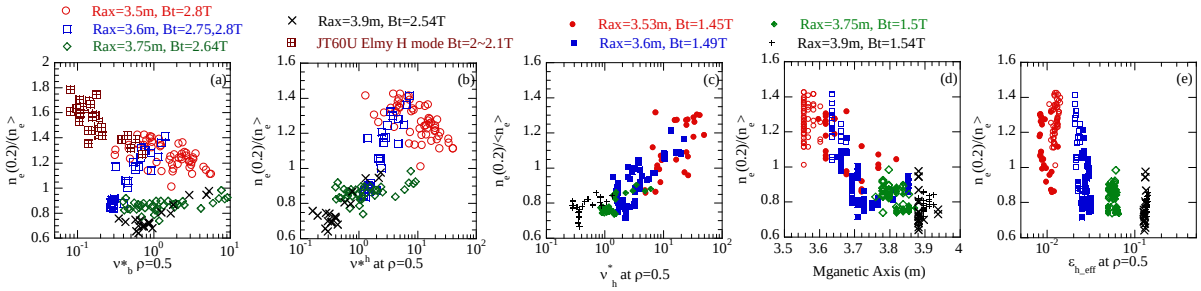

Fig.2 Parameter dependence of density peaking factor (a) comparison between LHD and JT60U, comparison between four configuration of LHD at (b) high filed and (c) low filed, dependence on (d) shifted magnetic axis position and (e) effective helical ripple

Data set of four configurations (Rax=3.5, 3.6, 3.75 and 3.9m) contained different ν^*_h and corresponding different peaking factor. At both high field (Fig.2 (b)) and low field (Fig.2 (c)), the density peaking factor was higher at more inward shifted configuration, where neoclassical transport was smaller. At the lower magnetic filed, density peaking factor was smaller and peaking factor depends more clearly on ν^*_h. As shown in Fig. 1 (d), density profile becomes more hollow at lower field. And the hollow density profile can be due to neoclassical outward convection [3]. One possible interpretation is, at lower field, the contribution of neoclassical can became larger.

Figure 2 (d) shows peaking factor dependence on shifted magnetic axis. The appropriate magnetic flux surface was selected for the Abel inversion and mapping for Thomson scattering. The axis position is at the vertical cross section. One important thing is the data of Fig.2 (d) included both low and high filed. The peaking factor of shifted data of Rax=3.53m at 1.45T was close to the peaking factor of Rax=3.75m at 2.64T. This indicates that the shifted inward configuration is equivalent to the outward shifted configuration without Shavranov shift.

Figure 2 (e) shows dependence on effective helical ripple (eq.(2)). The effective helical ripple was calculated taking into account for the finite beta effects [11]. Most of the data of LHD in Fig.2 are in plateau regime, where ν^*_h is larger than unity. Although the effective helical ripple is representative ripple in $1/\nu$ regime, the effective helical ripple played a role on density profile as well as global energy confinement [2]. However, as shown in Fig.2 (e), the density peaking varies at almost same ε_{eff}. Other hidden parameter should exist to determine density profile.

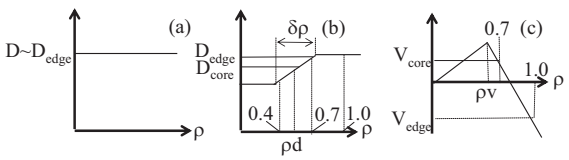

Fig.3 Assumed profile of D and V. (a) spatially constant D for localized modulation amplitude (b) two variable D for core sensitive case and (c) two variable V for all cases

2.2 Parameter dependence of particle transports

Particle transport in LHD was studied from density modulation experiments [3,4]. The diffusion coefficient (D) and convection velocity (V) were determined to fit modulation amplitude, phase and background density profiles [3,4]. Figure 3 shows the model used for the fitting. When modulation frequency is high or diffusion coefficient low, model of spatially constant D was used as shown in Fig.3 (a). When modulation penetrated deeper to core, two diffusion coefficient model was used as shown in Fig.3 (b).

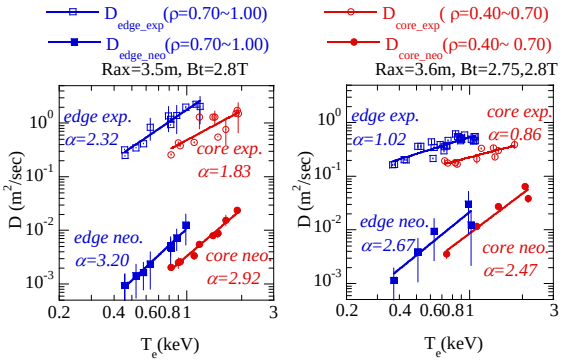

Fig. 4 Electron temperature dependence of diffusion coefficient (a) Rax=3.5m, Bt=2.8T and (b) Rax=3.6m ,Bt=2.75,2.8T. Dcore_exp, Dedge_exp are experimentally estimated core and edge diffusion coefficient. Dcore_neo, Dedge_neo are neoclassical values calculated by DCOM. Error bar of experimental values are fitting error, error bar of neoclassical values are standard deviations at ρ=0.4~0.7 for core value, and at ρ=0.7~1-.0 for edge value. T_e is also averaged at ρ=0.4~0.7 for core value, and at ρ=0.7~1-.0 for edge value.

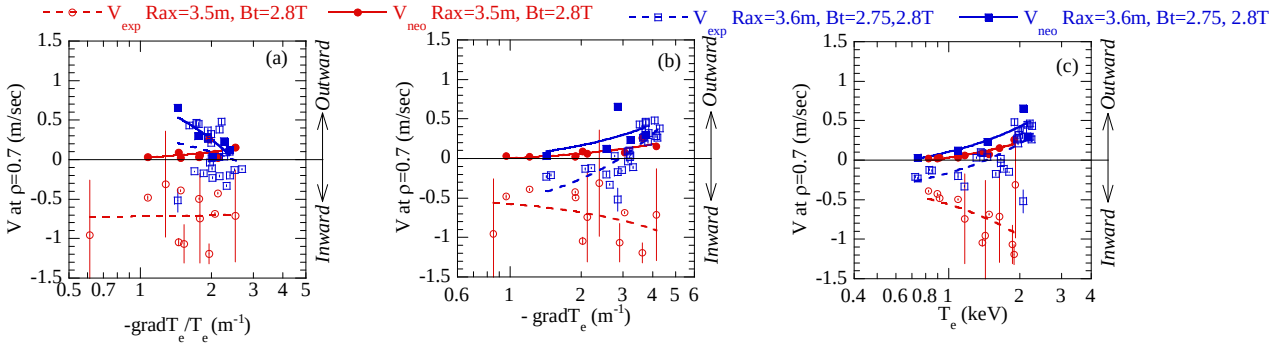

Fig.5 Dependence of Vcore (at ρ=0.7) on (a) normalized T_e gradient, (b) T_e gradient and (c) T_e. normalized T_e gradient, T_e gradient and T_e are averaged value at ρ =0.4~0.7.

In the model of Fig.3 (b), the diffusion coefficient transit at ρ=ρd with transition with δρ. The convection velocity was assumed to be zero at plasma center and to increase linearly and change slope at ρ=ρv. The value of ρd was fixed to be 0.7 for all cases. For Rax=3.5m, Bt=2.8T, δρ was fixed to 0.6 and , ρv was fixed to be 0.5. For other configuration, when modulation penetrated deeper to core, δρ was fixed to 0.3 and ρv was fixed to be 0.5. In order to compare with previous results [3,4], D_{edge} was D_{core}, V_{edge} and V_{core} was defined as follows. The spatial constant D was used as a D_{edge}, since the modulation amplitude was localized in the edge region. D_{core} and D_{edge} were defined the averaged value between ρ =0.4 and 0.7 and between ρ =0.7 and 1.0 respectively for the two values model of D. V_{core} and V_{edge} was defined as the value at ρ=0.7 and ρ=1.0 respectively.

Figure 4 shows the T_e dependence of D_{core} and D_{edge}. Neoclassical values calculated by DCOM[1] are also shown. The fitted lines are $A \times T_e^{\alpha}$, where A is a proportional factor and α is an exponent. Neoclassical values are smaller at Rax=3.5m than at Rax=3.6m at same T_e. However, experimental estimated D_{core} and D_{edge} were larger at Rax=3.5m than at 3.6m. Clear difference of T_e dependence of both neoclassical and anomalous D was also observed. The exponent of both neoclassical and experimental D_{core} and D_{edge} were larger at Rax=3.5m than at Rax=3.6m. At Rax=3.5m, the exponent of D_{core_neo} were factor 1.6 larger than at D_{core_exp} and exponent of D_{eddge_neo} were factor 1.4 larger than D_{core_exp}. At Rax=3.6m, the exponent of D_{core_neo} were factor 2.6 larger than at D_{core_exp} and exponent of D_{eddge_neo} were factor 2.6 larger than D_{core_exp}. At Rax=3.6m, large difference of the exponent between neoclassical and anomalous D were observed. This suggests the neoclassical D will be close to experimental D at higher T_e at Rax=3.6m .

Figure 5 shows comparison of parameter dependence of V_{core} of neoclassical and experimental values. The neoclassical particle flux is given by the following equation [12].

$$\Gamma_{e\_neo} = -nD_1\left\{\frac{\nabla n_e}{n_e} + \frac{eE_r}{T_e} + \left(\frac{D_2}{D_1} - \frac{3}{2}\right)\frac{\nabla T_e}{T_e}\right\} \quad (4)$$

The off diagonal term of the eq.(4) is convective flux, then , neoclassical convection velocity was defined by the following equation.

$$V_{e\_neo} = -D_1\left\{\frac{eE_r}{T_e} + \left(\frac{D_2}{D_1} - \frac{3}{2}\right)\frac{\nabla T_e}{T_e}\right\} \quad (5)$$

The data set used in this article was in the transition region or ion root region. In equation (4), the contribution of radial electric field on convection velocity was small and neoclassical convection was dominated by thermo diffusion term, which is the second term of eq.(5). As shown in Fig. 5, at Rax=3.6m, when convection velocity was outward directed and density profile was hollow, experimental convection velocity was comparable with neoclassical convection. This is same as the case of Rax=3.75, and 3.9m [3]. The clear T_e dependence of V_{core} was observed as shown in Fig.5 (c). So, the electron temperature is likely to be determine V_{core} as well as D

2.3 Configuration dependence of neoclassical and anomalous particle transport coefficient

There is an expectation that neoclassical optimization minimize anomalous transport simultaneously [2]. This is supported by theoretical work. In the single helicity heliotron configuration, smaller helical ripple configuration can generate larger zonal flow and can stabilize turbulence effectively [13]. The configuration dependence of particle transport coefficients are shown in Fig. (6) about high field case, and in Fig.7 about low field case.

Since both diffusion coefficients and convection velocity depends on T_e as described in the previous section, for the comparisons between different configurations, the values at the same Te were connected. As shown in Fig. 6 (a) and (b), at high field, the minimum of neoclassical D is

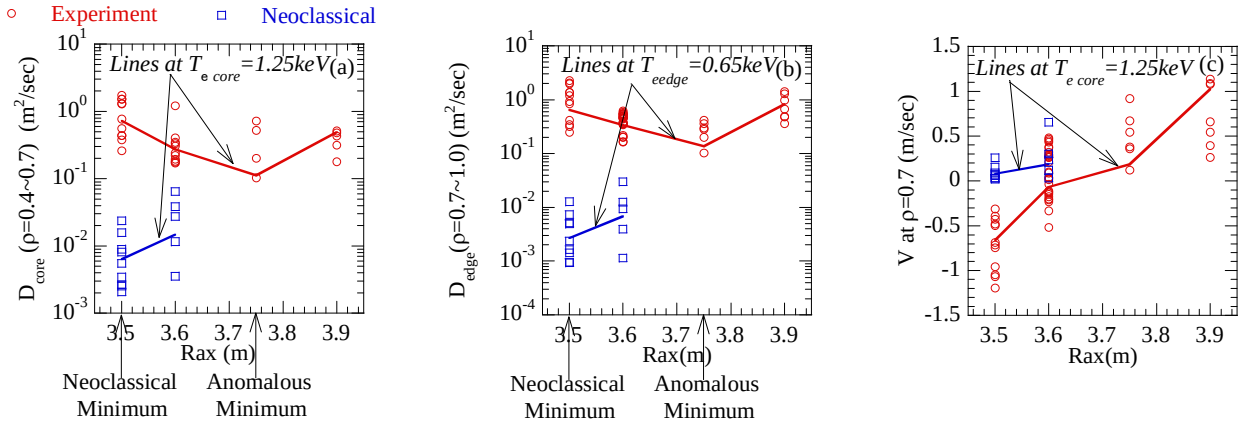

Fig.6 Comparison between neoclassical and anomalous transport coefficients at high field (a) Dcore, (b) Dedge and (c) Vcore at high filed (Bt=2.8T for Rax=3.5m,Bt=2.75, 2.8T for Rax=3.6m, Bt=2.64T for Rax=3.75m, Bt=2.54T for Rax=3.9m) Red and blue lines indicate the values at the same temperature. Neoclassical values were calculated by DCOM code[1]

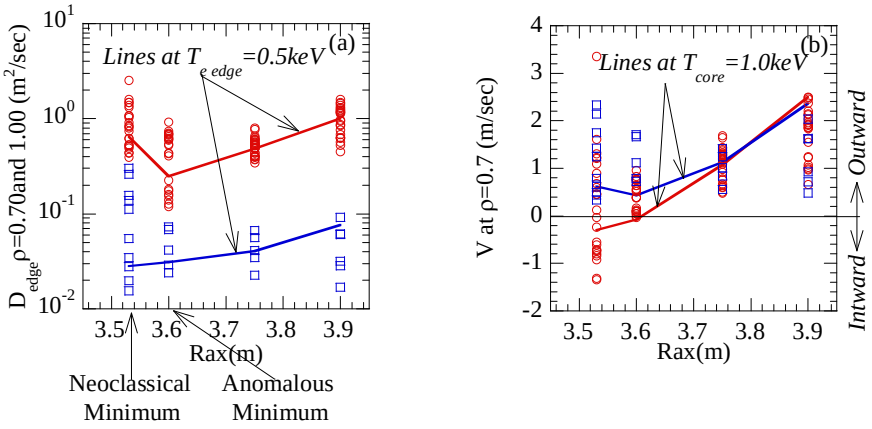

Fig.7 Comparison between neoclassical and anomalous transport coefficients at high field (a) Dedge and (c) Vcore at low filed (Bt=1.45T for Rax=3.53m,Bt=1.49T for Rax=3.6m, Bt=1.5T for Rax=3.75m, Bt=1.54T for Rax=3.9m) Red and blue lines indicate the values at the same temperature. Neoclassical values were calculated by GSRAKE code[14]

at Rax=3.5m, however experimental D was minimum at Rax=3.75m. On the other hand as shown in Fig.7 (a), at low field, neoclassical D_{edge} was minimum at Rax=3.53m, but experimental D_{edge} was minimum at Rax=3.6m. There are difference of the minimum configuration between neoclassical and anomalous particle diffusivity. The core convection both at high field and at low field became smaller at more inward shifted configuration. However, inward directed convection cannot be explained by neoclassical calculation.

2.3 Possible role of turbulence on density profile

The inward directed pinch in tokamak was widely observed and cannot be explained by ware pinch when collisional frequency becomes smaller [8,15]. The role of ITG/TEM turbulence was suggested [8,16]. In heliotron configuration, recently, theoretical work was done to investigate role of ITG/TEM turbulence[17]. In ref. 17, the direction of the quasi linear particle flux was estimated for the peaked and hollow density profile for the magnetic configuration of LHD. When density profile was hollow quasi linear particle flux was directed inward, then, as density profile becomes peaked, the direction of fluctuation driven particle flux reversed to outward. Since, particle source was negligible in the core region, particle flux should be zero. Possible interpretation of the role of fluctuation is as follows.

When density profile was hollow, particle flux driven by ITG/TEM turbulence was inward directed. This inward directed particle flux can be balanced with outward directed neoclassical convection to satisfy the particle balance. This is consistent with the results that diffusion was anomalous and outward convection was comparable with neoclassical when density profile was hollow [3].

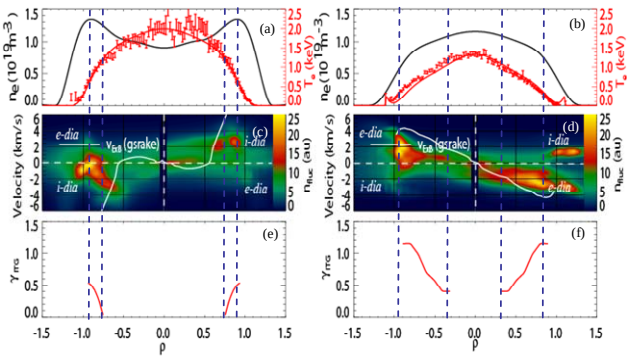

Fig.8 Comparison of (a), (b) n_e and T_e profile and (c), (d) fluctuation amplitude profile (k=0.1~0.6mm^{-1}) and (e), (f) ITG/TEM linear growth rate calculated by GOBLIN code [17]

When density profiles are peaked, particle flux can be driven by turbulence only. This is also consistent both diffusion and inward convection was anomalous for peaked density profiles.

Turbulence was measured by two dimensional phase contrast imaging [18,19] for hollow and peaked density profile. As shown in Fig.8, clear difference of fluctuation amplitude was observed. The linear growth rate of ITG/TEM turbulence was calculated by the GOBLIN code [17]. As shown in Fig.8 (c), (d), dominant part of turbulence existed at the location where linear growth rate was positive as shown in Fig. 8 (e), (f). Figure 8 (c) and (d) showed fluctuation amplitude only. The turbulence driven particle flux cannot be measured by using phase contrast imaging. However, observed fluctuation can possibly drive inward directed particle flux at hollow density profile and zero flux for peaked density profile.

3. Summary

The parameter dependence of density profile and particle transport was studied in the wide range of operational regime of LHD. Two different dependence on ν^*_b of density peaking factor was found. One is the gradual increase of peaking factor with reduction of ν^*_b at Rax=3.5m, 2.8T, where neoclassical transport minimum in the dataset. This is similar with tokamak behavior. The other is decrease of peaking factor with decrease of ν^*_b. This is observed in the other configuration and is particular in LHD. Smaller neoclassical may result in tokmak like behavior. The electron temperature dependences of D and V were investigated at around optimum neoclassical configuration at Rax=3.5m, 2.8T, and Rax=3.6m, 2.75,2.8T. The diffusion coefficient was one order magnitude larger than neoclassical value at both configurations, however, T_e dependence was different. At Rax=3.5m, 2.8T, T_e dependence was stronger than ones at Rax=3.6m, 2.75, 2.8T. At neoclassical minimum configuration (Rax=3.5m, 2.8T), the convection velocity at ρ = 0.7 was inward direction, which was not predicted by neoclassical theory. On the other hands, at Rax=3.6m, 2.75,2.8T, the convection velocity at ρ = 0.7 was inward directed at lower T_e and reverse to outward direction at higher T_e. When the convection velocity was outward directed, it was comparable with neoclassical value. These indicates, at neoclassical minimum configuration (Rax=3.5m, 2.8T), both diffusion and convection was determined by the anomalous process, but at Rax=3.6m, 2.75,2.8T, diffusion process was determined by the anomalous process, however convection was determined by neoclassical process at higher T_e. The present results shows neoclassical minimum is not same as anomalous minimum. The difference of the spatial profile of turbulence was observed, which suggested role of ITG/TEM turbulence on density profile

Acknowledgements

This work was supported by the National Institute for Fusion Science budget NIFS05ULHH511.

References

[1] S. Murakami et al Nucl. Fusion **42** (2002) L19–L22
[2] H.Yamada et al. Nucl. Fusion, **45**, 1684 (2005)
[3] K. Tanaka et al, FUSION SCIENCE AND TECHNOLOGY **51** 97 JAN. (2007)
[4] K. Tanaka *et al*., Nucl. Fusion **46** (2006) 110.
[5] K. Tanaka *et al*., to be submitted to PFR.
[6] K. Narihara *et al*., Rev. Sci. Instrum. **72** (2001) 1122.
[7] H. Takenaga, K. Tanaka, K. Muraoka et al., to be submitted Nucl. Fusion
[8] Angioni *et al*., Phys. Plasmas **10** (2003) 3225
[9] K. Miyamoto published by Iwanami Book Service Centre, Tokyo 1997 Fundamentals of Plasma Physics and Controlled Fusion.
[10] C. D. Beidler and W.N.G. Hitchon, Plasma Phys. Control. Fusion **36** (1994) 317.
[11] M.Yokoyama at al., *Journal of Plasma and Fusion Research*, **81**,83, (2005)
[12] V.Tribaldos,, *Phys. Plsama **8**, 1229, (2001)*
[13] H.Sugama, T-H. Watanabe, *Phys. Plasmas* **13**, 012501, (2006)
[14] C.D. Beidler and W.D. D'haeseleer, *Plasma Phys. Control. Fusion* **37** 463 (1995)
[15] Hoang G.T. *et al* 2003 *Phys. Rev. Lett.* **90** 155002-1
[16] Hoang G.T. *et al* 2004 *Phys. Rev. Lett.* **93** 135003-
[17] O. Yamagishi *et al*., Phys. Plasmas **14** (2007) 012505.
[18] C. Michael et al., Rev. Sci. Instrum. **77**, 10E923-1(2006)
[19] C. Michael et al.,to be published, Journal of Plasma and Fusion Research